DOI 10.5162/Ultrasonic2025/P1.16

Construction of a high-frequency ultrasonic flow-through chamber for emulsion and suspension separation

E.J Ramírez González[1], C.M Giraldo Atehortua [1], T.F. de Oliveira [1], L.O V. Pereira [2], J. H. Lopes[3], M. S.G. Tsuzuki[1], and F. Buiochi[1]
[1]Universidade de São Paulo, Department of Mechatronics Engineering Escola Politécnica, São Paulo, Brazil
[2] Petrobras, CENPES, Rio de Janeiro, Brazil
[2]Universidade Federal de Alagoas, Campus Arapiraca, Maceió, Brazil
eduardo1@usp.br

Abstract: High-frequency standing field can use the produced acoustic radiation force to separate and/or manipulate droplets and/or particles in liquids. While recent research has focused on microfluidics, there still remains a gap regarding the design parameters and characterization of large-scale, flow-through acoustic separation devices. Experimental validation demonstrated the formation of ultrasonic standing wave bands and the separation of oil-in-water emulsions. Simulation and experimental results showed consistent similarities.

Keywords: High-frequency ultrasound, acoustic separation, chamber design, oil-in-water emulsion, cornstarch suspension.

Introduction

Ultrasonic standing waves have been widely studied for particle manipulation and emulsion/suspension separation in microfluidic acoustophoresis and macroscale chambers [1]. High-frequency stationary ultrasonic fields generate acoustic radiation forces [2], which drive particles in liquids toward pressure nodal or antinodal planes. These forces enhance phase separation in acoustic chambers containing emulsions and suspensions [3]. Using ultrasound in the high kilohertz to low megahertz range is appealing due to its ability to control particles with minimal deformation and lower energy consumption compared to other methods [4]. Although recent studies have explored the fundamentals of acoustic standing waves in microfluidic systems, gaps remain in the design and characterization of large-scale, flow-through acoustic separators. Promising applications include the food, petrochemical, pharmaceutical, and biomedical sectors [5].

The resonating chamber design is critical for ultrasonic separators. Large chambers produce parallel nodal planes using a piezoelectric element bonded to a carrier layer. This assembly emits sound into a liquid-holding cavity, or active volume, which is bounded by a reflector. The cavity's resonant frequency depends on the sound speed in the active volume, which is temperature-dependent [6].

The present work presents the design of a high-frequency flow-through chamber for emulsion and suspension separation with six ultrasonic transducers of 1MHz. Working in the resonant frequencies of the cavity is crucial to maintain the standing wave inside the chamber, which may be altered by temperature or other parameters [6], therefore, a frequency tracking strategy was implemented to overcome the sound speed variation inside the active volume due to its temperature variation [7] .

Theory

Sound is an oscillating pressure wave that propagates through a medium with a specific frequency. When an ultrasound field is applied to a fluid containing suspended particles, they are influenced by the acoustic radiation force generated by wave scattering on the particles [8]. A standing wave forms from the reflection of a sound wave off a wall or a second transducer, resulting from the superposition of two propagating waves. This creates constructive interference, producing regions of maximum pressure amplitude (antinodes) and regions of zero pressure (nodes) [5].

Acoustic radiation force is categorized into primary and secondary components. The primary force acts along the wave propagation direction and drives particles toward nodes or antinodes of a standing wave. The secondary force clusters particles and helps maintain their positions. The primary radiation force (PRF) is given by [9]

$$F_r = -\left(\frac{\pi p_0^2 V_c}{2\lambda\rho_0 c_0^2}\right)\phi\sin(2kx). \qquad (1)$$

This force is proportional to the square of the acoustic pressure amplitude p_0^2 and the particle volume V_c. Here, x is the droplet position relative to a pressure node, λ the acoustic wavelength, k the wavenumber,

DOI 10.5162/Ultrasonic2025/P1.16

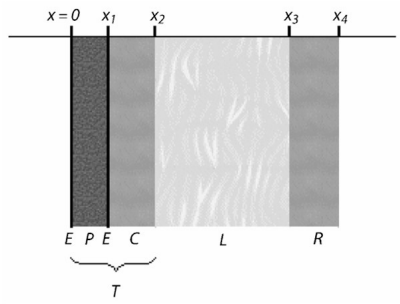

Fig. 1: Layered resonator and parts [6].

and c_0 the speed of sound in the fluid. The force strongly depends on particle size. Note also that pressure amplitude scales with applied voltage in piezoceramics. The acoustic contrast factor ϕ is defined as [9]

$$\phi = \frac{5\rho_d - 2\rho_0}{2\rho_d + \rho_0} - \frac{\rho_0 c_0^2}{\rho c_d^2}, \tag{2}$$

where ρ_d and c_d are the droplet's density and sound speed, respectively. The sign of ϕ—determined by the relative densities and sound speeds of the droplet and fluid—dictates force direction: droplets with positive ϕ migrate to pressure nodes, while those with negative ϕ move to antinodes.

The goal in designing and assembling the chamber is to efficiently transfer acoustic energy into the fluid. Fig. 1 shows a simple stack of plane-parallel layers: a piezoelectric element (P) bonded to a carrier layer (C). Together, they form the transducer (T), which emits an acoustic signal into the cavity containing the suspension liquid (L), also called the active volume (AV). This volume is bounded by a reflector (R) on the opposite side, which must remain parallel to the carrier to generate a standing wave [6].

PZT (lead-zirconate-titanate) ceramics, especially "hard" types, are commonly used as piezoelectric elements due to their strong ultrasonic output and high electro-mechanical coupling, particularly when the plate thickness is near multiples of a half wavelength. The reflector layer typically has high acoustic impedance (i.e., hard and dense), and its thickness should also be a multiple of $\lambda/2$ [10]. The active volume length is usually a multiple of $\lambda/2$ [11]. In multi-wavelength resonators, maintaining the driving frequency is essential, as temperature changes alter the speed of sound and thus the wavelength [12]. Turbulence, the main mechanism for flow across nodal planes, becomes more likely as dimensions increase [6].

Method and materials

A 136 cm^3 active volume chamber with six 1 MHz PZT piezoceramic plates (40×20×2 mm) was built,

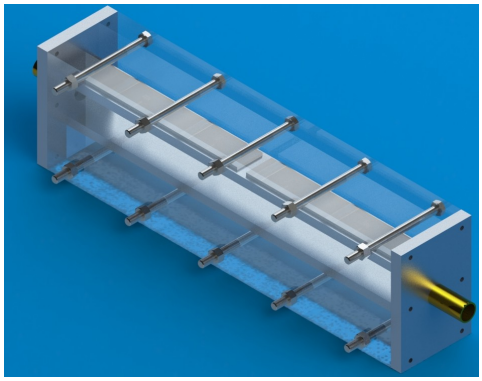

Fig. 2: Render of ultrasonic separation chamber.

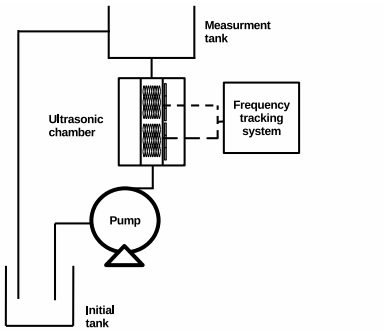

Fig. 3: Experimental circuit.

as illustrated in Fig. 2. The PZTs were bonded with conductive epoxy (EPO-TEK H20E) to a 6.4 mm aluminum coupling layer (approximatelly 2×λ/2) to generate standing waves in a 20 mm cavity, bounded by a parallel aluminum reflector of equal thickness. Acrylic plates allowed sample visualization, and both ends were sealed with aluminum plates featuring 9.2 mm inlet and outlet ports. To verify resonance, the chamber was characterized using an impedance analyzer (E5061 Keysight). Acoustic pressure simulations with water were performed in COMSOL Multiphysics 6.2, modeling piezoelectric, electric, and acoustic coupling.

Flow-through acoustic separation tests were conducted using a cornstarch suspension (9 g in 1800 cm^3 water) and a synthetic oil-in-water microemulsion with 3000 ppm oil (10 g petroleum, 9 g surfactant, 3000 cm^3 water at 80°C). Oil content was measured with an HD-1000 oil-in-water analyzer. Both tests ran at 40 W, 100 mL/min flow rate, and 30 minutes of ultrasound exposure. A resonance tracking system compensated for frequency shifts from temperature-induced sound speed variations. The experimental circuit diagram is shown in Fig. 3.

DOI 10.5162/Ultrasonic2025/P1.16

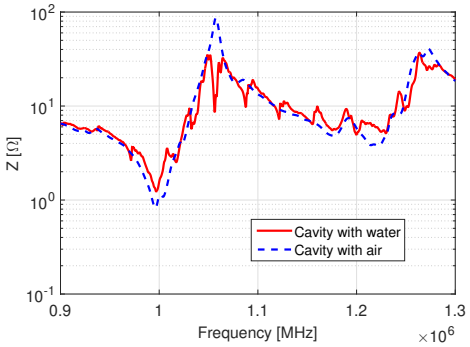

Fig. 4: Impedance of ultrasonic separation chamber.

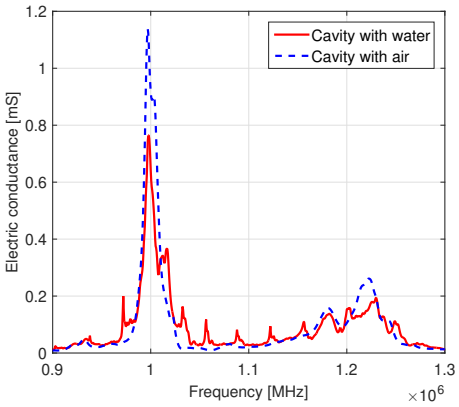

Fig. 5: Conductance of ultrasonic separation chamber.

Results and discussion

The constructed chamber was characterized by measuring impedance and conductance with and without water, as shown in Fig. 4 and Fig. 5. The piezoceramic resonance appears near 1MHz—as a low-impedance peak in Fig. 4 and a conductance peak in Fig. 5. The small peaks are attributed to the cavity. The presence of fluid introduces additional peaks from standing wave resonances, which shift with temperature.

A 2D COMSOL simulation was used to analyze standing wave pressure distribution across frequencies. Materials included aluminum, water, and PZT-4. Interfaces applied were pressure acoustics, frequency domain, solid mechanics, and electrostatics, with couplings for acoustic-structure boundary and piezoelectric effect. The fluid domain was meshed at $\lambda/8$ and given 0.2dB/m attenuation; the piezoelectric damping factor was set to 1×10^{-8}. Simulated impedance is shown in Fig. 6 alongside the experimental curve.

Fig. 6 shows that most resonance peaks align in frequency between simulation and experiment, though simulated amplitudes are higher—likely due to unmodeled attenuation in the experimental setup. The first flow-through acoustic separation test used the corn-

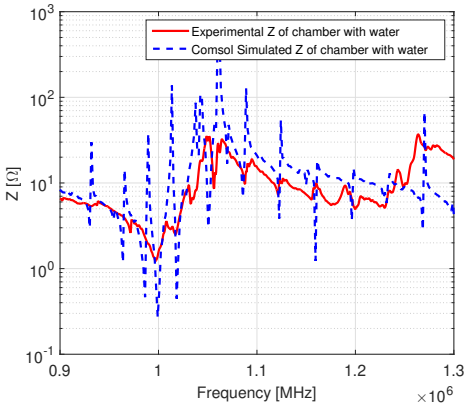

Fig. 6: Impedance of the ultrasonic chamber.

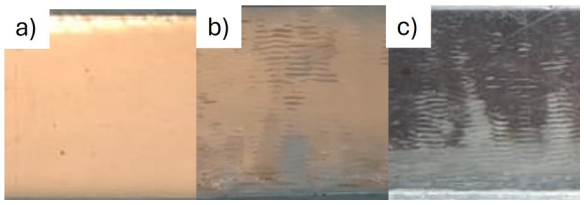

Fig. 7: Cornstrach separation test. a) Ultrasound OFF, b) Ultrasound ON, c) Treated water.

starch suspension. Upon ultrasound activation, particles rapidly agglomerated in a pattern that matched the simulations. Over time, cornstarch settled at the cavity bottom, leaving visibly clearer water (see Fig. 7). Although the operation remained stable, turbulence near the fluid inlet increased at flow rates of 500–1000 cm^3/min, which hindered particle agglomeration. Simulated and experimental standing wave patterns are shown in Fig. 8. A second experiment used a 3000 ppm synthetic oil-in-water microemulsion, with six tests—three with 30-minute ultrasound exposure and three without. Results are shown in Fig. 9 and Tab. 1.

Since the microemulsion was initially at approximately 55°C, early measurements were taken in a stirred tank since the pump operates below 45°C. Once cooled, measurements continued at the ultrasonic chamber outlet. Despite similar trends (Fig. 9), results show that ultrasonic treatment achieves faster

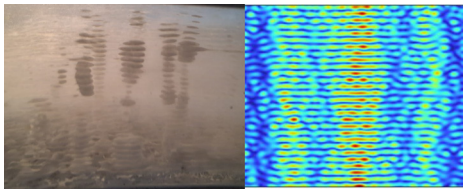

Fig. 8: Pressure pattern inside cavity.

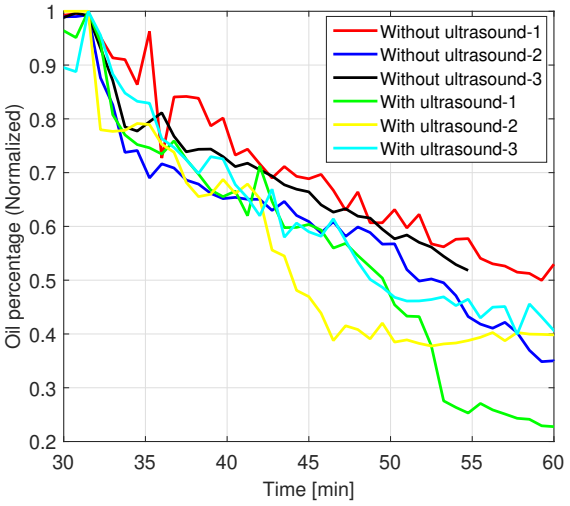

Fig. 9: Oil separation over time.

Tab. 1: Oil separation efficiency

Ultrasound	Ini. (PPM)	Fin.(PPM)	Separ (%)
Off 1	2354	1448	38%
Off 2	2053	1378	33%
Off 3	2067	1378	33%
On 1	2080	709.7	66%
On 2	2339	1133	52%
On 3	2650	1358	49%

and higher separation efficiency.

The results shown in Tab. 1 were obtained by measuring the petroleum content before and after a 20-minute acoustic treatment. In the absence of ultrasound, the average separation was 35%, in contrast, ultrasound application increased the average separation to 55%, with a maximum value of 66%. This corresponds to an improvement of approximately 36% relative to the condition without ultrasound.

Conclusions

A high-frequency ultrasonic flow-through chamber was designed, built, characterized, and tested for emulsion and suspension separation. Ultrasound effectively enhanced separation, as validated by simulations and impedance measurements. In oil-in-water emulsions, separation improved by approximatelly 36% over baseline. However, high inlet flow rates caused turbulence, reducing efficiency by disrupting droplet clustering—emphasizing the need to optimize both flow and acoustic conditions. Future studies will explore flow rate and power variations to identify optimal settings. Overall, results confirm ultrasound as a scalable method for improving separation in flow-through systems, with applications in wastewater treatment and oil recovery.

Acknowledgements

The authors acknowledge Petrobras/ANP (grants 5850.0109314.18.9 and 5850.0108871.18.9), CAPES, and CNPq (grants 306.123/2022-3 and 312.126/2021-2) for their financial support to this research.

References

[1] F. J. Trujillo et al. "Separation of suspensions and emulsions via ultrasonic standing waves - A review". In: *Ultrason Sonochem*. Vol. 21. 2014, pp. 2151–2164.

[2] X. Luo et al. "Phase separation technology based on ultrasonic standing waves: A review". In: *Ultrason Sonoch* 48 (2018), pp. 287–298.

[3] G. D. Pangu and D. L. Feke. "Acoustically aided separation of oil droplets from aqueous emulsions". In: *Chem Eng Sci* 59 (15 2004), pp. 3183–3193.

[4] J. Mierez et al. "Recent advances of ultrasound applications in the oil and gas industry". In: *Ultrason Sonochem* 103 (2024).

[5] T. Leong et al. "Ultrasonic separation of particulate fluids in small and large scale systems: A review". In: *Ind Eng Chemistry Research* 52 (47 2013), pp. 16555–16576.

[6] J. J. Hawkes and S. Radel. "Acoustofluidics 22: Multi-wavelength resonators, applications and considerations". In: *Lab Chip* 13 (4 Feb. 2013), pp. 610–627. ISSN: 14730189. DOI: 10.1039/c2lc41206c.

[7] C. M. G. Atehortúa et al. "Design and Implementation of the Frequency Control in an Ultrasonic Break Water-in-Oil Emulsion Chamber". In: *Physics Proc* 70 (2015). 2015 ICU, pp. 42–45.

[8] H. Bruus. "Acoustofluidics 7: The acoustic radiation force on small particles". In: *Lab Chip* 12 (6 2012), pp. 1014–1021.

[9] T. Laurell, F. Petersson, and A. Nilsson. "Chip integrated strategies for acoustic separation and manipulation of cells and particles". In: *Chem Soc Rev* 36 (3 2007), pp. 492–506.

[10] L. Kinsler et al. *Fundamentals of Acoustics*. Wiley, 2000. ISBN: 9780471847892.

[11] A. Lenshof et al. "Acoustofluidics 5: Building microfluidic acoustic resonators". In: *Lab Chip* 12 (4 2012), pp. 684–695.

[12] M. Greenspan and C. E. Tschiegg. "Tables of the Speed of Sound in Water". In: *J Acoust Soc Am* 31 (1).